HHS Public Access

Author manuscript

Genesis. Author manuscript; available in PMC 2021 May 10.

Published in final edited form as:

Genesis. 2021 March ; 59(3): e23412. doi:10.1002/dvg.23412.

Atypical protein kinase C is essential for embryonic vascular development in mice

Zee Chen[#1], **Yaoyun Duan**[#1], **Hong Wang**[1], **Huayuan Tang**[1], **Shijia Wang**[1], **Xinru Wang**[1], **Jie Liu**[2], **Xi Fang**[3], **Kunfu Ouyang**[1]

[1]Department of Cardiovascular Surgery, Peking University Shenzhen Hospital, School of Chemical Biology and Biotechnology, State Key Laboratory of Chemical Oncogenomics, Peking University Shenzhen Graduate School, Shenzhen, China

[2]Department of Pathophysiology, School of Medicine, Shenzhen University, Shenzhen, China

[3]Department of Medicine, School of Medicine, University of California San Diego, La Jolla, California

[#] These authors contributed equally to this work.

Summary

The atypical PKC (aPKC) subfamily constitutes PKCζ and PKCλ in mice, and both aPKC isoforms have been proposed to be involved in regulating various endothelial cell (EC) functions. However, the physiological function of aPKC in ECs during embryonic development has not been well understood. To address this question, we utilized Tie2-Cre to delete PKCλ alone (PKCλ-SKO) or both PKCλ and PKCζ (DKO) in ECs, and found that all DKO mice died at around the embryonic day 11.5 (E11.5), whereas a small proportion of PKCλ-SKO mice survived till birth. PKCλ-SKO embryos also exhibited less phenotypic severity than DKO embryos at E10.5 and E11.5, suggesting a potential compensatory role of PKCζ for PKCλ in embryonic ECs. We then focused on DKO embryos and investigated the effects of aPKC deficiency on embryonic vascular development. At E9.5, deletion of both aPKC isoforms reduced the diameters of vitelline artery and vein, and decreased branching from both vitelline vessels in yolk sac. Ablation of both aPKC isoforms also disrupted embryonic angiogenesis in head and trunk at the same stage, increasing apoptosis of both ECs and non-ECs. Taken together, our results demonstrated that aPKC in ECs plays an essential role in regulating cell apoptosis, angiogenesis, and embryonic survival.

Correspondence Xi Fang, Department of Medicine, University of California San Diego, 9500 Gilman Drive, La Jolla, CA, 92093-0613C. xifang@health.ucsd.edu, Kunfu Ouyang, School of Chemical Biology and Biotechnology, State Key Laboratory of Chemical Oncogenomics, Peking University Shenzhen Graduate School, Shenzhen, China, 518055. ouyang_kunfu@pku.edu.cn.

AUTHOR CONTRIBUTIONS

Zee Chen, Yaoyun Duan, Hong Wang, Huayuan Tang, Shijia Wang, and Xinru Wang: performed the experiments. Xi Fang and Kunfu Ouyang: designed the research. Zee Chen, Jie Liu, Xi Fang, and Kunfu Ouyang: wrote the manuscript.

CONFLICT OF INTEREST

The authors declare no conflicts of interest.

DATA AVAILABILITY STATEMENT

The data that support the findings of this study are available from the corresponding author upon reasonable request.

Keywords

angiogenesis; atypic protein kinase C; embryonic development; endothelial cell; vascular development

1 | INTRODUCTION

The protein kinase C (PKC) is a family of Ser/Thr kinases, which are divided into classical, novel, and atypical subfamilies, based on structure and sequence homology. In mammals, there are two atypical PKC (aPKC) genes, *Prkci* and *Prkcz*, in which *Prkci* encodes PKCλ in mice or PKCι in human, and *Prkcz* encodes a full-length protein PKCζ or at least one additional transcript PKMζ that skips the first four exons of the *Prkcz* gene (Drummond & Prehoda, 2016; Hapak, Rothlin, & Ghosh, 2019; Moscat, Diaz-Meco, & Wooten, 2009). The full-length proteins of PKCλ and PKCζ are highly related, sharing over 70% amino acid identity (Newton, 1997), both of which contain four functional domains including a unique PB1 domain at the N-terminus (Sumimoto, Kamakura, & Ito, 2007), a pseudosubstrate sequence that keeps the kinase inactive but posed for activation (Graybill, Wee, Atwood, & Prehoda, 2012), a C1 domain composed of a single cysteine rich zinc-finger motif which is considered as atypical due to the lack of specific amino acid residues of the phorbol ester-binding pocket (Ways, Cook, Webster, & Parker, 1992), and a kinase domain in the C-terminus which has very high degree of homology among various PKC isoforms (Hirai & Chida, 2003). Compared with classical and novel PKCs, aPKC contains only a single C1 domain that aPKC cannot bind to Ca^{2+}, diacylglycerol, and phorbol esters (Ways et al., 1992).

It has been shown that aPKC may regulate multiple cellular processes including polarity, migration, differentiation, and proliferation (Fogh, Multhaupt, & Couchman, 2014; Harris & Peifer, 2007). PKCλ is indispensable for embryonic survival. Deletion of PKCλ in mice results in early embryonic lethality by embryonic day 9.5 (E9.5), likely because of defects in development observed as early as E6.5 (Seidl et al., 2013; Soloff, Katayama, Lin, Feramisco, & Hedrick, 2004). However, PKCζ knockout mice are born in Mendelian ratios (Leitges et al., 2001). In endothelial cells (ECs), both PKCλ and PKCζ have been shown to play important regulatory roles. In embryoid bodies, ablation of PKCλ causes defects in directional EC migration and network assembly (Qi et al., 2011). PKCλ phosphorylates the clathrin-associated sorting protein Dab2, the transmembrane protein ephrin-B2, and the cell polarity regulator PAR-3, which further promotes VEGF receptor internalization and the angiogenic growth of vascular beds in newborn mouse retina. Deletion of PKCλ thus inhibits the size and complexity of retinal vascular network (Nakayama et al., 2013). On the other hand, PKCζ may regulate the expression of intercellular adhesion molecule-1 (ICAM-1) in ECs induced by tumor necrosis factor-α (TNFα), and thus regulate adhesion of leukocytes to ECs (Javaid et al., 2003). Furthermore, PKCζ can be activated by disturbed flow in ECs and has been proposed as a proapoptotic factor in ECs (Garin et al., 2007; Heo et al., 2011; Magid & Davies, 2005). However, the physiological function of aPKC in ECs during embryonic development remains unknown. To address this question, we here generated two mouse models with single deletion of PKCλ (PKCλ-SKO) or double deletion

of both PKCλ and PKCζ (DKO) in embryonic ECs by Tie2-Cre, and demonstrated an essential role of endothelial aPKC in regulating embryonic vascular development and survival. Our results also revealed a limited compensatory role of PKCζ for PKCλ in ECs during embryonic development.

2 | RESULTS

2.1 | Deletion of aPKC by Tie2-Cre resulted in embryonic lethality

To investigate the physiological function of aPKC in ECs during embryonic development, we first generated floxed *Prkci* and *Prkcz* heterogygous mice by targeting the exon 9 and 10 of mouse *Prkci* gene and the exon 10 of mouse *Prkcz* gene, respectively (Figure 1a,b). To delete PKCλ in ECs, we crossed male *Tie2-Cre*$^{+}$ *Prkci*$^{f/+}$ *Prkcz*$^{+/+}$ mice with *Prkci*$^{f/f}$ *Prkcz*$^{+/+}$ mice to generate *Tie2-Cre*$^{+}$ *Prkci*$^{f/f}$ *Prkcz*$^{+/+}$ (PKCλ-SKO) mice (Figure 1c). On the other hand, we crossed male *Tie2-Cre*$^{+}$ *Prkci*$^{f/+}$ *Prkcz*$^{f/f}$ mice with *Prkci*$^{f/f}$ *Prkcz*$^{f/f}$ mice to generate *Tie2-Cre*$^{+}$ *Prkci*$^{f/f}$ *Prkcz*$^{f/f}$ (DKO) mice (Figure 1d).

It has been shown that global deletion of PKCλ causes early embryonic developmental defects that can be observed as early as E6.5, and leads to embryonic lethality by E9.5 (Seidl et al., 2013; Soloff et al., 2004). We then investigated whether deletion of PKCλ in ECs could affect embryonic survival. In the offspring, we found only two PKCλ-SKO mice that survived to the postnatal day 10 (P10) and were fertile in adulthood, accounting for about 1.7% instead of the estimated 25% of the total pups, suggesting that most PKCλ-SKO mice died in the prenatal or perinatal stages (Table 1). We then set up timed mating and found that PKCλ-SKO embryos were observed at Mendelian ratios at E9.5, E10.5, and E11.5. At E9.5, no obvious morphological difference could be observed between PKCλ-SKO and control embryos (Figure 2a). However, most PKCλ-SKO embryos (6 off 7) at E10.5 were growth retarded, and the majority of PKCλ-SKO embryos (5 off 8) were dead and absorbed at E11.5 (Figure 2b–d; Table 1), suggesting that most PKCλ-SKO embryos, even not all, were embryonic lethal at around E11.5. Given that PKCζ has been proposed to partially compensate the role of PKCλ in embryonic development (Seidl et al., 2013), we then examined whether deletion of both PKCλ and PKCζ could cause a more profound developmental phenotype. Consistently, we found all DKO embryos were severely growth retarded at E10.5, and were dead and absorbed at E11.5 with no exception (Figure 2b–d; Table 2). We also found no DKO mice after birth (Table 2). Taken together, these results implicated a potential redundant role between PKCλ and PKCζ in ECs during embryonic development even though PKCλ may play a predominant role.

2.2 | Ablation of aPKC in endothelial cells disrupted embryonic vascular development

Considering that DKO embryos had more consistent embryonic phenotypes than PKCλ-SKO embryos, we then focused on DKO embryos and investigated how deletion of aPKC in ECs affected embryonic development. We first checked the vasculature of yolk sac at E9.5 when no obvious morphological changes could be found in DKO embryos. Yolk sac constitutes a honeycomb-like network of vessels undergoing rapid morphological changes to support the growing embryo. The primitive capillary plexus of yolk sac is established by about E8.5, and then these vessels expand and fuse to form large major vessels including

vitelline artery and vein (Garcia & Larina, 2014; Udan, Culver, & Dickinson, 2013). By performing whole-mount CD31 fluorescence immunostaining, we found that the architecture of vessels in DKO yolk sac was not apparently disrupted, evidenced by that the major vitelline arteries and veins were normally formed, and the branches were generated and well separated along the vitelline artery or the vein (Figure 3a). However, the diameters of both vitelline arteries and veins were significantly reduced in DKO yolk sac when compared with control yolk sac (Figure 3a,b). The numbers of branches from both vessels were also significantly decreased in DKO yolk sac (Figure 3c). We also examined the effect of aPKC deficiency on embryonic vascular development at the same stage, and found that deletion of aPKC caused disruption of vascular patterning in most embryo's regions including the head and the trunk. At E9.5, the vasculature was normally organized in a hierarchical pattern in control embryos, in which the first order branches were formed along the main vessels including the internal carotid artery of head, the cardinal vein of middle trunk, and the umbilical vein of caudal trunk, and well separated with each other. Furthermore, the secondary branches were also produced from the first order branches in these regions with their ends forming a vascular plexus (Figure 3d). However, the development of such a hierarchical pattern was delayed or disrupted in DKO embryos at the same stage. In DKO embryos, more first order branches could be observed along the main vessels but not well separated. In fact, most first order branches in DKO embryos were still connected as a vascular plexus, and no apparent secondary branches could be observed in the same regions (Figure 3d). Taken together, these results clearly demonstrated that aPKC in ECs is essential for normal vascular development in mouse embryo and yolk sac.

2.3 | Deletion of aPKC induced cell apoptosis in embryonic endothelial cells

We next investigated the effects of aPKC deficiency on EC apoptosis and proliferation. By performing immunofluorescence staining of cleaved-Caspase 3 and CD31 in E9.5 control and DKO embryos, we found that deletion of both aPKC isoforms increased cell apoptosis in both ECs and non-ECs. In E9.5 control embryos, the rate of apoptotic cells in either ECs or non-ECs was lower than 1%, indicating that only very few ECs or non-ECs underwent cell apoptosis at this stage. However, the rate of apoptotic cells in DKO EC and non-ECs in DKO embryos was about 4 and 13%, respectively (Figure 4a,b), indicating that deletion of both aPKC isoforms might induce apoptosis in ECs. On the other hand, cell proliferation of ECs and non-ECs was also assessed by immunofluorescence staining of phospho-Histone H3 and CD31 in control and DKO embryos at the same stage. However, we did not observe any significant difference in proliferation of ECs and non-ECs between control and DKO embryos at E9.5 (Figure 4c,d).

3 | DISCUSSION

In the present study, we demonstrated that aPKC in ECs is required for vascular development and survival in mouse embryos. The embryonic vascular system develops to afford the demands of the growing oxygen and nutrients for developing embryos. During embryonic development, ECs must be specified and assembled or added into growing vessels either through vasculogenesis, the de novo formation of vessels from aggregated endothelial precursors, or angiogenesis, the formation of neovessels from existing vessels

(Udan et al., 2013). The vascular plexus is extended and modified by a series of morphogenic processes, including new capillaries formation by sprouting and nonsprouting angiogenesis, small and large vessels remodeled from pre-existing vascular plexus, and the pruning of blood vessels (Risau, 1997). Abnormalities in vascular development have been recognized as one of major causes of embryonic growth delay or death of the fetus (Papaioannou & Behringer, 2012). In our present study, we found that deletion of both PKCλ and PKCζ in ECs decreased the size and branches of vitelline vessels in yolk sac and disrupted the architecture of embryo's vasculature at E9.5, which might be the primary cause of embryonic lethality of DKO embryos at E11.5. On the other hand, the vast majority of studies proposed that PKCλ and PKCζ play different and even opposite physiological functions even though these two aPKC isoforms are structurally highly related and share an overall amino acid identity of over 70% (Akimoto et al., 1994; Selbie, Schmitz-Peiffer, Sheng, & Biden, 1993). In our present study, we also generated a mouse model with single deletion of PKCλ in ECs, and provided the evidence that PKCζ may play a limited redundant role for PKCλ in ECs in regulating embryonic development and survival even though the role of PKCλ is dominant.

It has been proposed that aPKC may play various regulatory roles in ECs and angiogenesis. First, aPKC may regulate the transcription of VEGF. It has been shown that aPKC may bind and phosphorylate the transcriptional factor SP1, which plays a significant role in inducing the expression of vascular permeability factor/VEGF (Pal, Claffey, Cohen, & Mukhopadhyay, 1998). Secondly, aPKC may also regulate VEGF receptor internalization in plasma membrane and downstream signal transduction. aPKC may phosphorylate Dab2, ephrin-B2, and Par3, and thus regulate the angiogenic growth of vascular beds. Loss of PKCλ in ECs reduces the densities of both ECs and branches, and inhibits the size and complexity of retinal vascular network (Nakayama et al., 2013). In addition, aPKC may play a role in modulating the signaling pathway of angiopoietin-1 (Ang-1) in ECs. It has been shown that Ang-1 can induce the formation of a complex formed of aPKC and beta-catenin at cell–cell junctions and at the leading edge of migrating ECs, further bringing Par3, Par6, and adherens junction proteins at the front of migrating cells to locally activate Rac1 in response to Ang-1, and thus regulate directed and collective EC migration during angiogenesis (Oubaha et al., 2012). Furthermore, aPKC may also play an important role in regulating vascular network assembly mediated by Cdc42 (Qi et al., 2011). Therefore, it will be worthy to determine in the future whether deletion of both aPKC isoforms could really affect VEGF expression, VEGF receptor endocytosis, and phosphorylation of SP1, Dab2, ephrin-B2, and Par3 in embryonic vascular ECs. It will also be very interesting to identify more potential substrates for aPKC by performing the phospho-proteomic analysis in cultured control and DKO ECs.

Our results also suggested that deletion of both aPKC isoforms increased EC apoptosis at E9.5. In fact, aPKC may play an antiapoptotic or proapoptotic role in different cell types. In NIH-3T3 cells, aPKC may regulate the activation of nuclear factor kappa-light-chain-enhancer of activated B cells (NFκB) signaling pathway. aPKC can be activated by TNFα and has been shown to be required for the activation of NFκB by this cytokine. Ectopically expressed or activated PKCλ is sufficient to trigger NFκB nuclear activity and the transcriptional activation (Diaz-Meco, Lallena, Monjas, Frutos, & Moscat, 1999). Moreover,

negative mutants of either PKCλ or PKCζ inhibit kappa B-dependent transcription and IKK activation (Lallena, Diaz-Meco, Bren, Paya, & Moscat, 1999). Considering that NFkB can upregulate various antiapoptotic genes and is essential for cell growth and survival (Jani, DeVecchio, Mazumdar, Agyeman, & Houghton, 2010; Karin & Lin, 2002), aPKC may thus play an antiapoptotic role in these cells. On the other hand, PKCζ can be activated by disturbed flow in ECs (Garin et al., 2007). PKCζ activation promotes apoptosis through TNFα-mediated JNK and caspase-3 activation in ECs (Garin et al., 2007). Moreover, PKCζ activation can also induce EC apoptosis through regulating p53 SUMOylation and p53-Bcl-2 binding (Heo et al., 2011). These studies strongly suggested that activation of PKCζ is a proapoptotic factor in ECs (Garin et al., 2007). Therefore, it will be very interesting to investigate in the future the molecular mechanisms underlying the regulation of aPKC in cell apoptosis of embryonic ECs.

In addition to embryogenesis, angiogenesis is also essential for tumor growth and metastasis. Controlling tumor-associated angiogenesis using either antibodies or tyrosine kinase inhibitors has been approved to treat several types of cancer (Lugano, Ramachandran, & Dimberg, 2020; Weis & Cheresh, 2011). Our present study clearly demonstrated that deletion of aPKC in ECs is sufficient to disrupt embryonic angiogenesis. Furthermore, deletion of PKCλ in ECs of newborn mice has also been shown to inhibit the size and complexity of retinal vascular network (Nakayama et al., 2013). On the other hand, it has been proposed that aPKC may also play important regulatory roles in tumorigenesis in numerous studies. In particular, PKCλ/ι is upregulated in most primary solid tumors and has been recognized as a tumor promoter (Garg et al., 2014; Murray, Kalari, & Fields, 2011; Reina-Campos, Diaz-Meco, & Moscat, 2019). By contrast, both upregulation and downregulation of PKCζ have been observed in human cancers, and is generally considered as a tumor suppressor (Dave et al., 2006; Galvez et al., 2009; Sanchez-Carbayo, Socci, Lozano, Saint, & Cordon-Cardo, 2006). Therefore, it will be very worthy to determine whether inhibition of aPKC activity using genetic manipulation or small molecular inhibitors could reduce tumor angiogenesis and growth in the future. Given that angiogenesis can also contribute to beneficial outcomes following focal ischemia in model systems (Kanazawa et al., 2019), it is also worthy to investigate whether aPKC plays a regulatory role in models of ischemic diseases.

4 | METHODS

4.1 | Mice

The *Prkcz* and *Prkci* floxed mice were generated using a similar strategy as previously described (Ouyang et al., 2014). Briefly, the *Prkcz* and *Prkci* mouse genomic DNA clones were isolated from a 129SVJ mouse genomic library and used to construct the *Prkcz* and *Prkci* targeting vector. Two fragments containing the exon 9 and 10 of *Prkci* and the exon 10 of *Prkcz* were inserted into two loxP sites in a targeting vector that contains a neomycin selection cassette flanked by two FRT sites, respectively. Targeting vectors were linearized by the restriction enzyme NotI and subsequently electroporated into R1 embryonic stem (ES) cells. G418-resistant ES clones were screened for homologous recombination by DNA blot analysis. Two independent homologous recombinant ES clones for each targeting

construct were microinjected into blastocysts from C57BL/6J mice to generate male chimeras. Male chimeras were bred with female Black Swiss mice to generate germline transmitted floxed heterozygous mice (*Prkcz*$^{+/\text{flox-neo}}$ and *Prkci*$^{+/\text{flox-neo}}$), which were further characterized with polymerase chain reaction (PCR) using two primers (P1 and P2) spanning the first LoxP site and two other primers (P3 and P4) spanning the first FRT site, respectively. Subsequently, *Prkcz*$^{+/\text{flox-neo}}$ and *Prkci*$^{+/\text{flox-neo}}$ were crossed with FLPe transgenic mice to remove the neomycin resistance cassette (Rodriguez et al., 2000). Afterward, *Prkci*$^{f/f}$ and *Prkci*$^{f/f}$*Prkcz*$^{f/f}$ mice were then generated and crossed the Tie2-Cre mice that express the Cre recombinase under the control of mouse endothelial-specific Tie2 promoter (Kisanuki et al., 2001), to generate *Tie2-Cre*$^{+}$*Prkci*$^{f/f}$ (PKCλ-SKO) and *Tie2-Cre*$^{+}$*Prkci*$^{f/f}$*Prkcz*$^{f/f}$ (DKO) mice, respectively. The littermate *Tie2-Cre*$^{-}$*Prkci*$^{f/f}$ and *Tie2-Cre*$^{-}$*Prkci*$^{f/f}$*Prkcz*$^{f/f}$ mice were used as control.

4.2 | DNA analysis

The genomic DNA was extracted from embryo's yolk sac or mouse tails, and PCR was used to identify the genotypes as previous described (Lin et al., 2019), using the following gene-specific primers (from 5′ to 3′): *Tie2-Cre* (forward, CCCTGTGCTCAGACAGAAATGAGA; reverse, CGCATAA CCAGTGAAACAGCATTGC), *Prkci* (forward, GCAGCAGTAGCTAGCCAACC; reverse, CATGAGG TCCCC TCCATTTA), and *Prkcz* (forward, GAGAGCGAACCCTGAAAGTG; reverse, CTGCACCCAGTCGATA TCCT).

4.3 | Morphological analysis

Embryos and yolk sacs were dissected from the maternal decidua under a Leica MZ6 dissecting light microscope at the indicated stage after a timed mating, with noon on the day of discovering a vaginal plug defined as E0.5, and then photographed as previously described (Wang et al., 2019).

4.4 | Immunostaining

Embryos were freshly collected at E9.5, fixed in 4% paraformaldehyde (PFA) diluted in phosphate buffered saline (PBS), incubated with an ascending series of sucrose concentrations from 5 to 20%, and embedded in optimal cutting temperature (OCT) compound (Sakura Finetek USA Inc., Torrance, California). Cryosections (7 μm) were prepared, and immunostaining was performed using CD31 (BD Pharmingen, catalog no. 550274), phospho-Histone H3 (Sigma, catalog no. 06–570), and cleaved-Caspase 3 antibody (catalog no. 9661; Cell Signaling Technologies) as previously described (Fan et al., 2020).

4.5 | Whole-mount immunofluorescence staining

Whole-mount immunofluorescence staining in yolk sac was performed as previously described (Duan et al., 2019). In brief, embryo's yolk sac was collected and fixed with 4% PFA at 4°C overnight, washed and incubated in the blocking buffer (2% bovine serum albumin, 5% horse serum in PBS containing 0.2% Triton X-100) for 1 hr at room temperature, followed by the incubation with anti-CD31 antibody (BD Pharmingen, catalog no. 550274) at 4°C overnight. Subsequently, the tissues were washed again for three times

and incubated with Alexa-conjugated secondary antibodies diluted with the blocking buffer for 1 hr at room temperature. Finally, the tissues were flat-mounted with Dako Fluorescent Mounting Media, and pictures were acquired under an Olympus 1 × 73 Fluorescence Microscopy.

4.6 | Whole-mount PECAM staining

Whole-mount PECAM staining in embryos was perform as previously described (Yang et al., 2020). First, embryos were collected at E9.5 and fixed in 4% PFA overnight at 4°C overnight, washed and dehydrated with a methanol series (25, 50, 75, and 100% methanol) for 15 min at room temperature. Next, the embryos were quenched with 5% hydrogen peroxide, washed twice with 100% methanol at room temperature, and subsequently rehydrated with 75, 50, and 25% methanol, and with PBS twice. After that, the embryos were incubated with the blocking buffer for several hours and then incubated with the primary CD31 antibody at 4°C overnight, followed by incubation with HRP-conjugated goat anti-rat IgG at 4°C overnight. At the end, 3′,3′-diaminobenzidine was used to develop the color, and pictures were acquired using a stereomicroscope.

4.7 | Statistics

The scatter plots were drawn using GraphPad Prism 5 as previously described (Lin et al., 2016). Statistical analysis was performed using a two-tailed, unpaired Student's *t* test. All data represents the mean ± *SEM* (error bars). The $p < .05$ was considered statistically significant.

4.8 | Study approval

All mice were housed under a 12-hr day/night cycle at a temperature of 25°C. All animal care and experiments were conducted in accordance with the guidelines established by the Animal Care and Use Committee (IACUC) at Peking University Shenzhen Graduate School (Shenzhen, China), and approved by the IACUC (Approval #: AP0017). Periodic review of procedures was performed, and amendments were made as needed.

ACKNOWLEDGEMENTS

The authors would like to thank Ju Chen (University of California, San Diego) for critical reading of our manuscript. This work was supported by the National Natural Science Foundation of China (31800767 to H.T., 81970421 to K.O.), the Shenzhen Basic Research Foundation (JCYJ20170818090044949 to H.T., JCYJ20190808174001746 to K.O.), the Guangdong Province Basic Research Foundation (2018A030310012 to H.T.), and the Shenzhen-Hong Kong Institute of Brain Science-Shenzhen Fundamental Research Institutions (2019SHIBS0004 to K.O.).

REFERENCES

Akimoto K, Mizuno K, Osada S, Hirai S, Tanuma S, Suzuki K, & Ohno S (1994). A new member of the third class in the protein kinase C family, PKC lambda, expressed dominantly in an undifferentiated mouse embryonal carcinoma cell line and also in many tissues and cells. Journal of Biological Chemistry, 269(17), 12677–12683.

Dave SS, Fu K, Wright GW, Lam LT, Kluin P, Boerma EJ, … Lymphoma/Leukemia Molecular Profiling Project. (2006). Molecular diagnosis of Burkitt's lymphoma. The New England Journal of Medicine, 354(23), 2431–2442. 10.1056/NEJMoa055759. [PubMed: 16760443]

Diaz-Meco MT, Lallena MJ, Monjas A, Frutos S, & Moscat J (1999). Inactivation of the inhibitory kappaB protein kinase/nuclear factor kappaB pathway by Par-4 expression potentiates tumor necrosis factor alpha-induced apoptosis. The Journal of Biological Chemistry, 274(28), 19606–19612. 10.1074/jbc.274.28.19606. [PubMed: 10391896]

Drummond ML, & Prehoda KE (2016). Molecular control of atypical protein kinase C: Tipping the balance between self-renewal and differentiation. Journal of Molecular Biology, 428(7), 1455–1464. 10.1016/j.jmb.2016.03.003. [PubMed: 26992354]

Duan Y, Wang H, Mitchell-Silbaugh K, Cai S, Fan F, Li Y, … Ouyang K (2019). Heat shock protein 60 regulates yolk sac erythropoiesis in mice. Cell Death & Disease, 10(10), 766. 10.1038/s41419-019-2014-2. [PubMed: 31601784]

Fan F, Duan Y, Yang F, Trexler C, Wang H, Huang L, … Ouyang K (2020). Deletion of heat shock protein 60 in adult mouse cardiomyocytes perturbs mitochondrial protein homeostasis and causes heart failure. Cell Death and Differentiation, 27(2), 587–600. 10.1038/s41418-019-0374-x. [PubMed: 31209364]

Fogh BS, Multhaupt HA, & Couchman JR (2014). Protein kinase C, focal adhesions and the regulation of cell migration. The Journal of Histochemistry and Cytochemistry, 62(3), 172–184. 10.1369/0022155413517701. [PubMed: 24309511]

Galvez AS, Duran A, Linares JF, Pathrose P, Castilla EA, Abu-Baker S, … Moscat J (2009). Protein kinase Czeta represses the interleukin-6 promoter and impairs tumorigenesis in vivo. Molecular and Cellular Biology, 29(1), 104–115. 10.1128/MCB.01294-08. [PubMed: 18955501]

Garcia MD, & Larina IV (2014). Vascular development and hemodynamic force in the mouse yolk sac. Frontiers in Physiology, 5, 308. 10.3389/fphys.2014.00308. [PubMed: 25191274]

Garg R, Benedetti LG, Abera MB, Wang H, Abba M, & Kazanietz MG (2014). Protein kinase C and cancer: What we know and what we do not. Oncogene, 33(45), 5225–5237. 10.1038/onc.2013.524. [PubMed: 24336328]

Garin G, Abe J, Mohan A, Lu W, Yan C, Newby AC, … Berk BC (2007). Flow antagonizes TNF-alpha signaling in endothelial cells by inhibiting caspase-dependent PKC zeta processing. Circulation Research, 101(1), 97–105. 10.1161/CIRCRESAHA.107.148270. [PubMed: 17525369]

Graybill C, Wee B, Atwood SX, & Prehoda KE (2012). Partitioning-defective protein 6 (Par-6) activates atypical protein kinase C (aPKC) by pseudosubstrate displacement. The Journal of Biological Chemistry, 287(25), 21003–21011. 10.1074/jbc.M112.360495. [PubMed: 22544755]

Hapak SM, Rothlin CV, & Ghosh S (2019). aPKC in neuronal differentiation, maturation and function. Neuronal Signaling, 3(3), NS20190019. 10.1042/NS20190019. [PubMed: 32269838]

Harris TJ, & Peifer M (2007). aPKC controls microtubule organization to balance adherens junction symmetry and planar polarity during development. Developmental Cell, 12(5), 727–738. 10.1016/j.devcel.2007.02.011. [PubMed: 17488624]

Heo KS, Lee H, Nigro P, Thomas T, Le NT, Chang E, … Abe J (2011). PKCzeta mediates disturbed flow-induced endothelial apoptosis via p53 SUMOylation. The Journal of Cell Biology, 193(5), 867–884. 10.1083/jcb.201010051. [PubMed: 21624955]

Hirai T, & Chida K (2003). Protein kinase Czeta (PKCzeta): Activation mechanisms and cellular functions. Journal of Biochemistry, 133(1), 1–7. 10.1093/jb/mvg017. [PubMed: 12761192]

Jani TS, DeVecchio J, Mazumdar T, Agyeman A, & Houghton JA (2010). Inhibition of NF-kappaB signaling by quinacrine is cytotoxic to human colon carcinoma cell lines and is synergistic in combination with tumor necrosis factor-related apoptosis-inducing ligand (TRAIL) or oxaliplatin. The Journal of Biological Chemistry, 285(25), 19162–19172. 10.1074/jbc.M109.091645. [PubMed: 20424169]

Javaid K, Rahman A, Anwar KN, Frey RS, Minshall RD, & Malik AB (2003). Tumor necrosis factor-alpha induces early-onset endothelial adhesivity by protein kinase Czeta-dependent activation of intercellular adhesion molecule-1. Circulation Research, 92(10), 1089–1097. 10.1161/01.RES.0000072971.88704.CB. [PubMed: 12714560]

Kanazawa M, Takahashi T, Ishikawa M, Onodera O, Shimohata T, & Del Zoppo GJ (2019). Angiogenesis in the ischemic core: A potential treatment target? Journal of Cerebral Blood Flow and Metabolism, 39(5), 753–769. 10.1177/0271678X19834158. [PubMed: 30841779]

Karin M, & Lin A (2002). NF-kappaB at the crossroads of life and death. Nature Immunology, 3(3), 221–227. 10.1038/ni0302-221. [PubMed: 11875461]

Kisanuki YY, Hammer RE, Miyazaki J, Williams SC, Richardson JA, & Yanagisawa M (2001). Tie2-Cre transgenic mice: A new model for endothelial cell-lineage analysis in vivo. Developmental Biology, 230(2), 230–242. 10.1006/dbio.2000.0106. [PubMed: 11161575]

Lallena MJ, Diaz-Meco MT, Bren G, Paya CV, & Moscat J (1999). Activation of IkappaB kinase beta by protein kinase C isoforms. Molecular and Cellular Biology, 19(3), 2180–2188. 10.1128/mcb.19.3.2180. [PubMed: 10022904]

Leitges M, Sanz L, Martin P, Duran A, Braun U, Garcia JF, … Moscat J (2001). Targeted disruption of the zetaPKC gene results in the impairment of the NF-kappaB pathway. Molecular Cell, 8(4), 771–780. 10.1016/s1097-2765(01)00361-6. [PubMed: 11684013]

Lin Q, Zhao G, Fang X, Peng X, Tang H, Wang H, … Ouyang K (2016). IP3 receptors regulate vascular smooth muscle contractility and hypertension. JCI Insight, 1(17), e89402. 10.1172/jci.insight.89402. [PubMed: 27777977]

Lin Q, Zhao L, Jing R, Trexler C, Wang H, Li Y, … Ouyang K (2019). Inositol 1,4,5-trisphosphate receptors in endothelial cells play an essential role in vasodilation and blood pressure regulation. Journal of the American Heart Association, 8(4), e011704. 10.1161/JAHA.118.011704. [PubMed: 30755057]

Lugano R, Ramachandran M, & Dimberg A (2020). Tumor angiogenesis: Causes, consequences, challenges and opportunities. Cellular and Molecular Life Sciences, 77(9), 1745–1770. 10.1007/s00018-019-03351-7. [PubMed: 31690961]

Magid R, & Davies PF (2005). Endothelial protein kinase C isoform identity and differential activity of PKCzeta in an athero-susceptible region of porcine aorta. Circulation Research, 97(5), 443–449. 10.1161/01.RES.0000179767.37838.60. [PubMed: 16051884]

Moscat J, Diaz-Meco MT, & Wooten MW (2009). Of the atypical PKCs, Par-4 and p62: Recent understandings of the biology and pathology of a PB1-dominated complex. Cell Death and Differentiation, 16(11), 1426–1437. 10.1038/cdd.2009.119. [PubMed: 19713972]

Murray NR, Kalari KR, & Fields AP (2011). Protein kinase Ciota expression and oncogenic signaling mechanisms in cancer. Journal of Cellular Physiology, 226(4), 879–887. 10.1002/jcp.22463. [PubMed: 20945390]

Nakayama M, Nakayama A, van Lessen M, Yamamoto H, Hoffmann S, Drexler HC, … Adams RH (2013). Spatial regulation of VEGF receptor endocytosis in angiogenesis. Nature Cell Biology, 15(3), 249–260. 10.1038/ncb2679. [PubMed: 23354168]

Newton AC (1997). Regulation of protein kinase C. Current Opinion in Cell Biology, 9(2), 161–167. 10.1016/s0955-0674(97)80058-0. [PubMed: 9069266]

Oubaha M, Lin MI, Margaron Y, Filion D, Price EN, Zon LI, … Gratton JP (2012). Formation of a PKCzeta/beta-catenin complex in endothelial cells promotes angiopoietin-1-induced collective directional migration and angiogenic sprouting. Blood, 120(16), 3371–3381. 10.1182/blood-2012-03-419721. [PubMed: 22936663]

Ouyang K, Leandro Gomez-Amaro R, Stachura DL, Tang H, Peng X, Fang X, … Chen J (2014). Loss of IP3R-dependent Ca2+ signalling in thymocytes leads to aberrant development and acute lymphoblastic leukemia. Nature Communications, 5, 4814. 10.1038/ncomms5814.

Pal S, Claffey KP, Cohen HT, & Mukhopadhyay D (1998). Activation of Sp1-mediated vascular permeability factor/vascular endothelial growth factor transcription requires specific interaction with protein kinase C zeta. The Journal of Biological Chemistry, 273(41), 26277–26280. 10.1074/jbc.273.41.26277. [PubMed: 9756852]

Papaioannou VE, & Behringer RR (2012). Early embryonic lethality in genetically engineered mice: Diagnosis and phenotypic analysis. Veterinary Pathology, 49(1), 64–70. 10.1177/0300985810395725. [PubMed: 21233329]

Qi Y, Liu J, Wu X, Brakebusch C, Leitges M, Han Y, … Li S (2011). Cdc42 controls vascular network assembly through protein kinase Ciota during embryonic vasculogenesis. Arteriosclerosis, Thrombosis, and Vascular Biology, 31(8), 1861–1870. 10.1161/ATVBAHA.111.230144.

Reina-Campos M, Diaz-Meco MT, & Moscat J (2019). The dual roles of the atypical protein kinase Cs in cancer. Cancer Cell, 36(3), 218–235. 10.1016/j.ccell.2019.07.010. [PubMed: 31474570]

Risau W (1997). Mechanisms of angiogenesis. Nature, 386(6626), 671–674. 10.1038/386671a0. [PubMed: 9109485]

Rodriguez CI, Buchholz F, Galloway J, Sequerra R, Kasper J, Ayala R, … Dymecki SM (2000). High-efficiency deleter mice show that FLPe is an alternative to Cre-loxP. Nature Genetics, 25(2), 139–140. 10.1038/75973. [PubMed: 10835623]

Sanchez-Carbayo M, Socci ND, Lozano J, Saint F, & Cordon-Cardo C (2006). Defining molecular profiles of poor outcome in patients with invasive bladder cancer using oligonucleotide microarrays. Journal of Clinical Oncology, 24(5), 778–789. 10.1200/JCO.2005.03.2375. [PubMed: 16432078]

Seidl S, Braun U, Roos N, Li S, Ludtke TH, Kispert A, & Leitges M (2013). Phenotypical analysis of atypical PKCs in vivo function display a compensatory system at mouse embryonic day 7.5. PLoS One, 8(5), e62756. 10.1371/journal.pone.0062756. [PubMed: 23690951]

Selbie LA, Schmitz-Peiffer C, Sheng Y, & Biden TJ (1993). Molecular cloning and characterization of PKC iota, an atypical isoform of protein kinase C derived from insulin-secreting cells. Journal of Biological Chemistry, 268(32), 24296–24302.

Soloff RS, Katayama C, Lin MY, Feramisco JR, & Hedrick SM (2004). Targeted deletion of protein kinase C lambda reveals a distribution of functions between the two atypical protein kinase C isoforms. Journal of Immunology, 173(5), 3250–3260. 10.4049/jimmunol.173.5.3250.

Sumimoto H, Kamakura S, & Ito T (2007). Structure and function of the PB1 domain, a protein interaction module conserved in animals, fungi, amoebas, and plants. Science's STKE, 2007(401), re6. 10.1126/stke.4012007re6.

Udan RS, Culver JC, & Dickinson ME (2013). Understanding vascular development. Wiley Interdisciplinary Reviews: Developmental Biology, 2(3), 327–346. 10.1002/wdev.91. [PubMed: 23799579]

Wang H, Jing R, Trexler C, Li Y, Tang H, Pan Z, … Ouyang K (2019). Deletion of IP3R1 by Pdgfrb-Cre in mice results in intestinal pseudo-obstruction and lethality. Journal of Gastroenterology, 54(5), 407–418. 10.1007/s00535-018-1522-7. [PubMed: 30382364]

Ways DK, Cook PP, Webster C, & Parker PJ (1992). Effect of phorbol esters on protein kinase C-zeta. Journal of Biological Chemistry, 267(7), 4799–4805.

Weis SM, & Cheresh DA (2011). Tumor angiogenesis: Molecular pathways and therapeutic targets. Nature Medicine, 17(11), 1359–1370. 10.1038/nm.2537.

Yang F, Huang L, Tso A, Wang H, Cui L, Lin L, … Ouyang K (2020). Inositol 1,4,5-trisphosphate receptors are essential for fetal-maternal connection and embryo viability. PLoS Genetics, 16(4), e1008739. 10.1371/journal.pgen.1008739. [PubMed: 32320395]

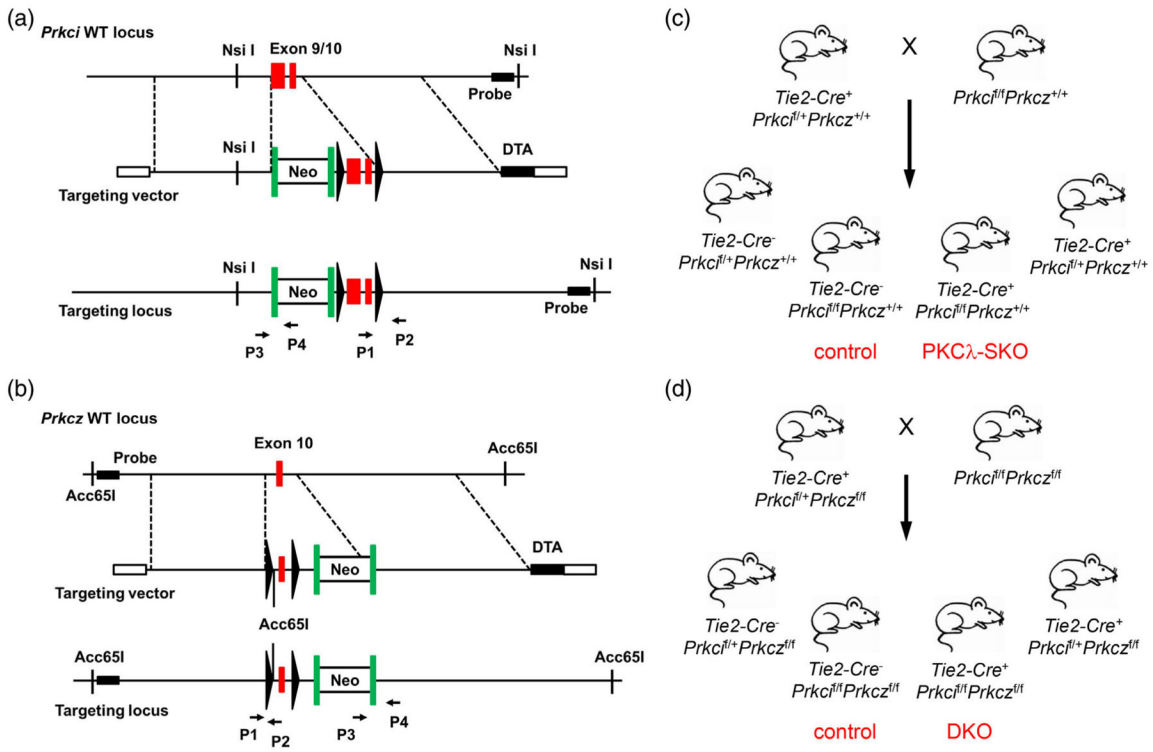

FIGURE 1.

Gene targeting and mouse breeding strategy. (a,b) Schematic diagram of gene targeting strategy for mouse *Prkci* and *Prkcz* genes. Genomic localization of the exon 9 and 10 of *Prkci* gene (red rectangles) and the exon 10 of *Prkcz* gene (top), the targeting constructs containing a neomycin cassette (Neo) flanked by two FRT sites (green rectangles) with the exon 9 and 10 of *Prkci* and the exon 10 of *Prkcz* floxed by two LoxP sites (black triangles), respectively (middle), and the floxed locus for mouse *Prkci* and *Prkcz* genes after homologous recombination (bottom). Nsi I and Acc65I represent the restriction enzymes. P1, P2, P3 and P4 indicate the location of PCR primers for genotypic analysis. (c) Schematic diagram of mouse breeding strategy to generate endothelial cell-specific PKCλ knockout mice. Male *Tie2-Cre*$^{+}$ *Prkci*$^{f/+}$ *Prkcz*$^{+/+}$ mice were crossed with female *Prkci*$^{f/f}$ *Prkcz*$^{+/+}$ mice to generate endothelial cell-specific PKCλ knockout (*Tie2-Cre*$^{+}$ *Prkci*$^{f/f}$ *Prkcz*$^{+/+}$; PKCλ-SKO) mice. The littermate with *Tie2-Cre*$^{-}$ *Prkci*$^{f/f}$ *Prkcz*$^{+/+}$ mice were used as control. (d) Schematic diagram of mouse breeding strategy to generate endothelial cell-specific PKCλ and PKCζ double knockout mice. Male *Tie2-Cre*$^{+}$ *Prkci*$^{f/+}$ *Prkcz*$^{f/f}$ mice were crossed with female *Prkci*$^{f/f}$ *Prkcz*$^{f/f}$ mice to generate *Tie2-Cre*$^{+}$ *Prkci*$^{f/f}$ *Prkcz*$^{f/f}$ (DKO) mice. The littermate with *Tie2-Cre*$^{-}$ *Prkci*$^{f/f}$ *Prkcz*$^{f/f}$ mice were used as control

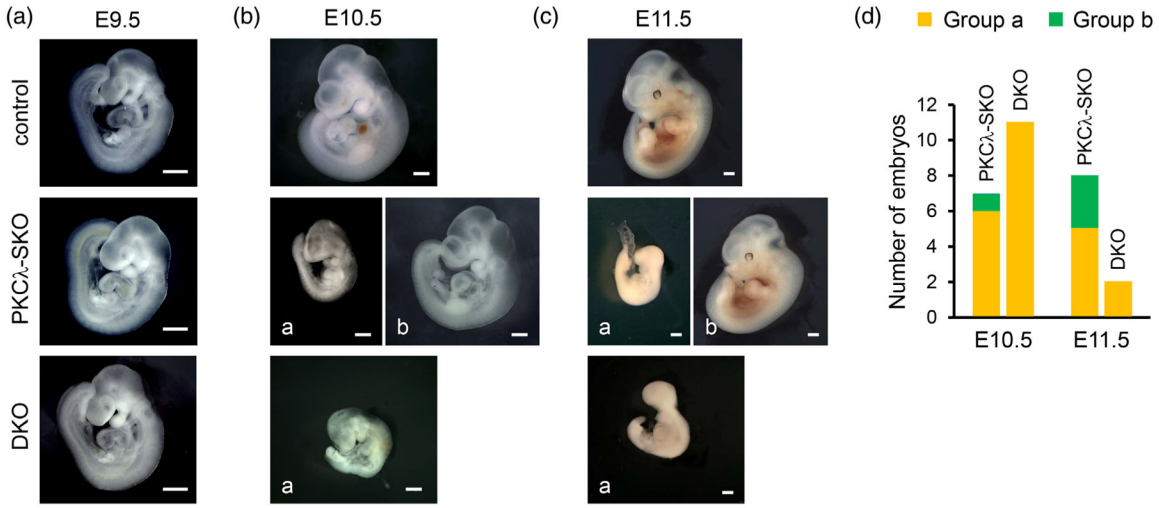

FIGURE 2.

Deletion of aPKC in endothelial cells resulted in embryonic lethality. (a–c) Representative images of control, PKCλ-SKO, and DKO embryos at E9.5 (a), E10.5 (b), and E11.5 (c). Please note that PKCλ-SKO embryos at E10.5 and E11.5 were subdivided into two groups, in which group a refers to the embryos with severe growth retardation at E10.5 and the embryos that were dead and absorbed at E11.5, and group b refers to the embryos that were not or only slightly growth retarded at E10.5 or E11.5. Scale bar, 500 μm. Please also note no DKO embryos could be classified into group b at both E10.5 and E11.5. (d) Number of group a and group b of SKO and DKO embryos at E10.5 and E11.5

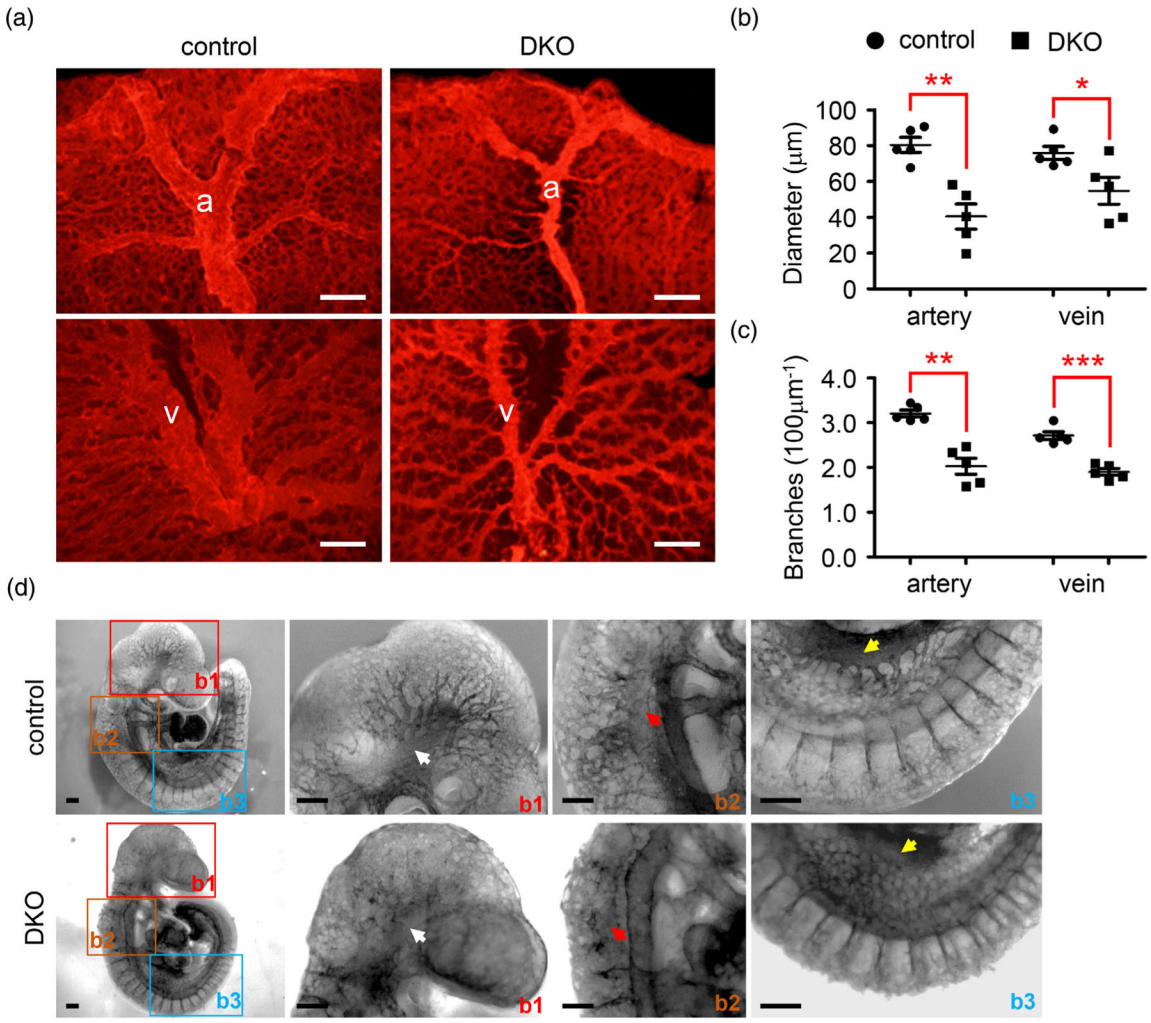

FIGURE 3.

Ablation of aPKC in endothelial cells disrupted embryonic vascular development. (a) Representative images of whole-mount immunofluorescence staining of CD31 in control and DKO yolk sacs at E9.5. a, vitelline artery; b, vitelline vein. Scale bar, 200 μm. (b,c) Quantification analysis of the diameter (b) and branches (c) of vitelline artery and vein in control and DKO yolk sac at E9.5. $n = 5$ for each group. All data represent mean ± *SEM*. Significance was determined by two-tailed, unpaired Student's *t* test. $*p < .05$, $**p < .01$, $***p < .001$ versus control. (d) Representative images of whole-mount PECAM/CD31 staining of control and DKO embryos at E9.5 at low and high magnifications. Please note a hierarchical vascular architecture in head (b1), middle trunk (b2), and caudal trunk (b3) of control embryo. The first order and secondary branches can be clearly seen from the internal carotid artery of head (white arrow), the cardinal vein of middle trunk (red arrow), and the umbilical vein (yellow arrow) in control embryo. Scale bar, 200 μm

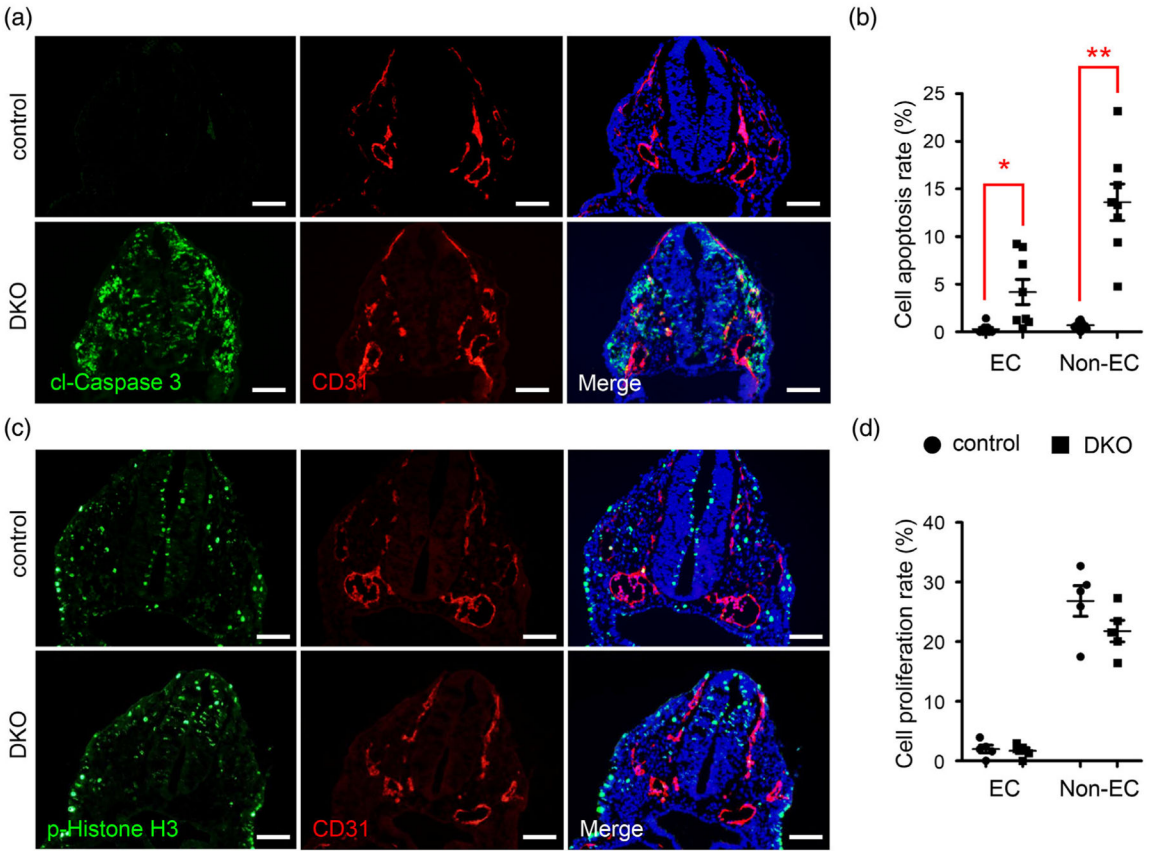

FIGURE 4.

Deletion of aPKC in endothelial cells increased cell apoptosis. (a) Representative images of immunofluorescences staining for cleaved-Caspase 3 (cl-Caspase 3) in embryonic section at E9.5, with endothelial cells co-stained with CD31. Scale bar, 200 μm. (b) Quantitative analysis of apoptosis in endothelial and nonendothelial cells. $n = 8$ per group. All data represent mean ± SEM. Significance was determined by two-tailed, unpaired Student's t test. *$p < .05$, **$p < .01$ versus control. (c) Representative images of immunofluorescences staining for phospho-Histone H3 (p-Histone H3) and CD31 in embryonic section at E9.5. Scale bar, 200 μm. (d) Quantitative analysis of proliferation in control and DKO endothelial and nonendothelial cells. $n = 5$ per group. All data represent mean ± *SEM*. Significance was determined by two-tailed, unpaired Student's t test

TABLE 1

Genotypic frequency of embryos and pups from the intercrosses *Tie2-Cre*$^{+}$ *Prkci*$^{f/+}$ *Prkcz*$^{+/+}$ X *Prkci*$^{f/f}$ *Prkcz*$^{+/+}$

Genotype Stage	*Tie2-Cre*$^{-}$, *Prkci*$^{f/+}$*Prkcz*$^{+/+}$	*Tie2-Cre*$^{-}$, *Prkci*$^{f/f}$*Prkcz*$^{+/+}$	*Tie2-Cre*$^{+}$, *Prkci*$^{f/+}$*Prkcz*$^{+/+}$	*Tie2-Cre*$^{+}$, *Prkci*$^{f/f}$*Prkcz*$^{+/+}$	Total
E9.5	25 (28.4)	21 (23.9)	20 (22.7)	22 (25.0)	88
E10.5	7 (22.6)	8 (25.8)	9 (29.0)	7 (22.6)[a]	31
E11.5	12 (34.2)	7 (20.0)	8 (22.9)	8 (22.9)[b]	35
P10	38 (32.5)	40 (34.2)	37 (31.6)	2 (1.7)[c]	117
Expected (%)	25	25	25	25	100

[a] About 6 of 7 mutant embryos were absorbed, while one of them was alive with heart beating.

[b] About 5 of 8 mutant embryos were absorbed, while three of them only exhibited slight growth retardation.

[c] Two mutant mice survived to adulthood and had reproductive ability.

TABLE 2

Genotypic analysis of embryos and pups from *Tie2-Cre*$^{+}$ *Prkci*$^{f/+}$ *Prkcz*$^{f/f}$ X *Prkci*$^{f/f}$ *Prkcz*$^{f/f}$ intercrosses

Genotype Stage	*Tie2-Cre*$^{-}$, *Prkci*$^{f/+}$*Prkcz*$^{f/f}$	*Tie2-Cre*$^{-}$, *Prkci*$^{f/f}$*Prkcz*$^{f/f}$	*Tie2-Cre*$^{+}$, *Prkci*$^{f/+}$*Prkcz*$^{f/f}$	*Tie2-Cre*$^{+}$, *Prkci*$^{f/f}$*Prkcz*$^{f/f}$	Total
E9.5	78 (28.1)	61 (21.9)	70 (25.2)	69 (24.8)	278
E10.5	27 (38.1)	17 (23.9)	16 (22.5)	11 (15.5)[a]	71
E11.5	6 (21.4)	10 (35.7)	10 (35.7)	2 (7.1)[b]	28
P10	43 (35.5)	45 (37.2)	33 (27.3)	0 (0.0)	121
Expected (%)	25	25	25	25	100

[a] All mutant embryos exhibited severe growth retardation.

[b] All mutant embryos were dead and absorbed.